Heat and Moisture Budgets of Tropical Mesoscale Anvil Clouds

RICHARD H. JOHNSON AND GEORGE S. YOUNG

Department of Atmospheric Science, Colorado State University, Fort Collins, CO 80523

(Manuscript received 21 March 1983, in final form 5 July 1983)

ABSTRACT

An analysis of the heat and moisture budgets of tropical mesoscale anvil clouds has been carried out. Mesoscale anvils, defined as widespread (~100 km) cloud systems extending from near the freezing level to the high troposphere, are characterized by light, stratiform precipitation. These cloud features, which are preceded by and generally merged with cumulonimbus clouds, are prevalent throughout the tropics and summertime midlatitudes and may account for an important fraction of the total tropical rainfall.

Sounding data from the December 1978 field phase of the International Winter Monsoon Experiment (Winter MONEX) are used to determine heat and moisture (Q_1 and Q_2) budgets for a number of mesoscale anvil cloud systems. The composite heating (Q_1) profile shows a warming peak in the upper troposphere near 350 hPa or 8–9 km that can be attributed to condensation and freezing in the anvil and a cooling peak in the lower troposphere near 700 hPa or 3 km due to rainfall evaporation and melting. The moisture (Q_2) budget shows a drying maximum in the upper troposphere coincident with the warming peak and a moistening maximum in the lower troposphere near 800 hPa or 2 km.

The heat budget is compared with that determined recently for mesoscale anvils by Houze (1982), who has used an independent and different approach, and good agreement between the two heating distributions is found. The heating and moistening profiles for mesoscale anvils are considerably different from those determined by large-scale budget studies of entire tropical cloud clusters, which contain both cumulonimbus and mesoscale anvil cloud effects. In particular, the heating profiles diagnosed here show an upward shift in the level of maximum heating, and *cooling*, instead of heating, in the lower troposphere, extending from near the freezing level to the surface.

1. Introduction

There is increasing evidence to indicate that a large proportion of the earth's precipitation is organized into mesoscale (~10–100 km) features characterized by groups or bands of convective cloud systems. This mesoscale organization is present almost everywhere: in extratropical cyclones, in summertime convection at midlatitudes and in convective systems in the tropics (see recent comprehensive reviews by Hobbs, 1978; Houze and Betts, 1981; and Houze and Hobbs, 1982). Convection in the latter two categories occurs in atmospheric environments that are conditionally unstable and, while differences exist, there are noted similarities in the mesoscale organization of convection between the tropics and midlatitudes (Houze and Hobbs, 1982). Information on the vertical heating distributions associated with deep convection organized on the mesoscale is just now becoming available (Houze, 1982). In this paper we attempt to add to this knowledge by investigating the tropospheric heating and moistening distributions within tropical mesoscale convective systems observed during the International Winter Monsoon Experiment (Winter MONEX).

In this study rawinsonde data from Winter MONEX are used to determine the apparent heat source Q_1 and apparent moisture sink Q_2 (after Yanai *et al.*, 1973) for the mesoscale cloud components of tropical cloud clusters. The mesoscale cloud structures discussed here, which will be hereafter referred to as *mesoscale anvils* following Brown (1979), are extensive (~100 km or greater) cloud systems having bases in the mid-troposphere near the 0°C level extending to near the tropopause. These anvils are characterized by a predominantly stratiform cloud and precipitation structure (Leary and Houze, 1979). They are prevalent throughout the tropics and summertime midlatitudes (Houze and Hobbs, 1982), and in the tropics may account for a significant portion of the total rainfall (estimated to be ~40% in GATE by Cheng and Houze, 1979). It is important to establish heating and moistening distributions associated with these types of cloud systems. Houze (1982) demonstrates that these distributions appear to be quite different from those for cumulus or cumulonimbus convection, the primary contributor to the remainder of the tropical rainfall. A proper partitioning of the total convective heating may be quite important for achieving improvements in the parameterization of cumulus convection in large-scale prediction models (Johnson, 1980; Houze *et al.*, 1980; Leary and Houze, 1980; Houze, 1982; Fritsch and Brown, 1982). The works of Anthes (1977) and Anthes and Keyser (1979) have demonstrated an important sensitivity of regional numerical prediction model simulations to the vertical distribution of convective heating as given by the cumulus parameterization scheme. Hartmann *et al.* (1983) also find a marked sensitivity of the equatorial Pacific Walker circulation to the assumed vertical distribution of convective heating. The heat and moisture budgets for mesoscale anvils reported in this study will hopefully contribute to an elucidation of the total convective heating field associated with tropical cloud clusters and consequently, to a better understanding of their impact on the large-scale circulation.

2. Winter MONEX mesoscale convective systems

A considerable amount of new information on the structure and properties of mesoscale convective systems has been gained during the past decade as a result of a number of comprehensive field programs in the tropics and at midlatitudes. From tropical experiments, particularly the GARP Atlantic Tropical Experiment (GATE), the internal cloud and precipitation structure of mesoscale convective systems has received detailed scrutiny for the first time (see review by Houze and Betts, 1981). Importantly, it has been found that tropical mesoscale convection in many areas of the world, whether squall or nonsquall in character, undergoes a similar pattern of evolution or life cycle behavior (Leary and Houze, 1979; Zipser *et al.*, 1981). This pattern is illustrated well by that occurring in the region of Winter MONEX over the South China Sea just to the north of Borneo (Fig. 1, adapted from Houze *et al.*, 1981).

Houze *et al.* (1981) and Johnson and Priegnitz (1981) have studied convection off the north coast of Borneo and found that during the December 1978

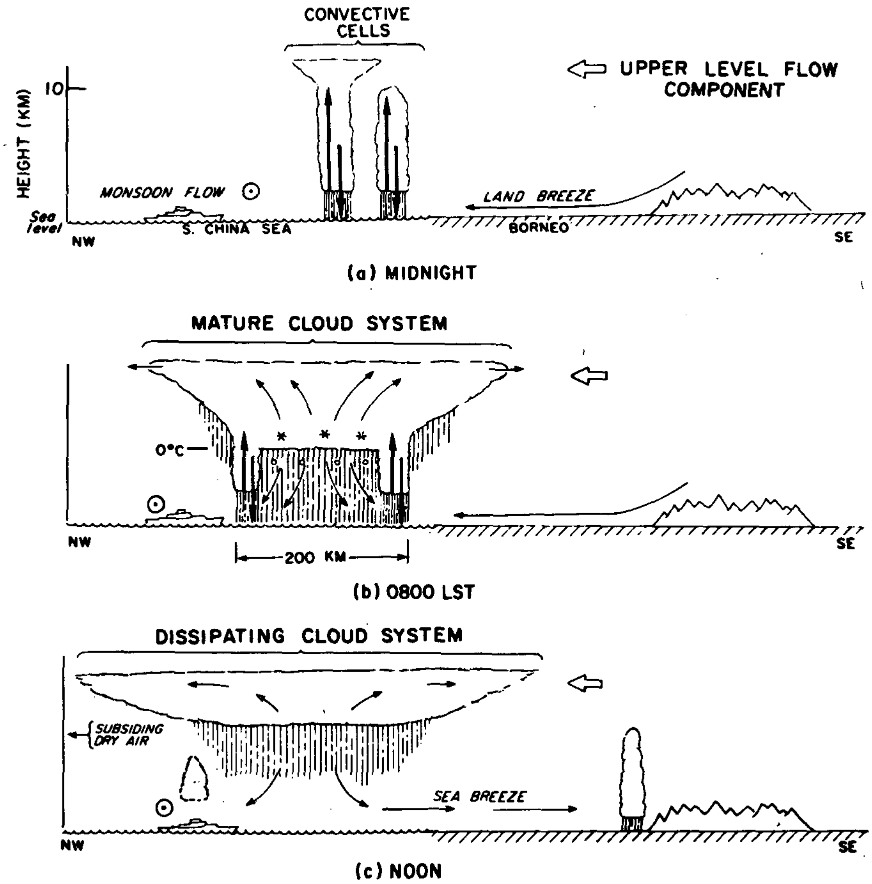

FIG. 1. Schematic of the development of diurnally generated nonsquall cloud cluster off the coast of Borneo. Various arrows indicate airflow. Circumscribed dot indicates northeasterly monsoon flow out of page. Outlined arrow indicates the component of the typical east-southeasterly upper-level flow in the plane of the cross section. Heavy vertical arrows in (a) and (b) indicate cumulus-scale updrafts and downdrafts. Thin arrows in (b) and (c) show a mesoscale updraft developing in a mid- to upper-level stratiform cloud with a mesoscale downdraft in the rain below the middle-level base of the stratiform cloud. Asterisks and small circles indicate ice above the 0°C level melting to form raindrops just below this level. Figure adapted from Houze *et al.* (1981).

field phase of Winter MONEX, mesoscale convective systems developed on a regular basis or nearly every day of the month. Initially these systems began as clusters of cumulonimbus clouds initiated around midnight by low-level convergence between the northeast monsoon flow over the South China Sea and the land breeze along the north coast of Borneo (Fig. 1, top). By sunrise the cumulonimbus convection had transformed into a mesoscale cloud system characterized by a stratiform cloud layer (mesoscale anvil) with a base in the mid-troposphere near the 0°C level from which light precipitation fell and with some remaining cumulonimbus on the periphery (Fig. 1, middle). Later, by midday, the mesoscale cloud system moved to the west-northwest in the direction of the upper-level flow and dissipated over the South China Sea in late afternoon (Fig. 1, bottom). The average speed of movement of the mesoscale anvil systems, estimated based on satellite data to be $\sim$6 m s^{-1} (Johnson and Priegnitz, 1981), is considerably less than the speed of the flow at many levels of the troposphere, thus indicating the Winter MONEX clusters are of nonsquall, rather than squall, character as defined by Zipser *et al.* (1981).

A number of studies of Winter MONEX convection have already been carried out. The radar precipitation and microphysical structure of the mesoscale cloud systems have been examined by Houze *et al.* (1981) and Churchill and Houze (1983). Webster and Stephens (1980) have investigated the possible impacts of their extensive cloud shields on the net radiative field of the tropics. Johnson and Priegnitz (1981), Johnson (1982) and Johnson and Kriete (1982) have studied the thermodynamic and circulation characteristics of the cloud systems, while Warner (1981, 1982), mainly using photographs taken from research aircraft, has documented cloud structures in and around the deep convective activity.

The existence of a triangular array of Soviet research ships with sounding capability in the path of many mesoscale convective systems during 6–28 December (Fig. 2) has provided a unique opportunity for the determination of their effects on the large-scale flow. Johnson (1982) has determined the vertical motion in and below Winter MONEX anvils when they passed the ship array in their mature to dissipating stages during the early afternoon (at 1400 LST). He found upward motion above cloud base with an average peak near 250 hPa (10 km) of $\sim$12 cm s^{-1} and downward motion below with a peak near 650 hPa (3.5 km) of ~ -3 cm s^{-1}. This profile of vertical motion closely resembles that determined recently by Gamache and Houze (1982) for the mesoscale anvil in a tropical squall line in GATE. It is considerably different from that for boundary-layer-rooted cumulonimbus clouds (e.g., see squall-line component vertical velocity in Fig. 13 of Gamache and Houze, 1982). The impact of these different circulations on the total convective heating in tropical cloud clusters has been recently examined by Houze (1982). This paper will also address this question by providing independent estimates of mesoscale anvil cloud convective heating that can be compared to those given by Houze (1982).

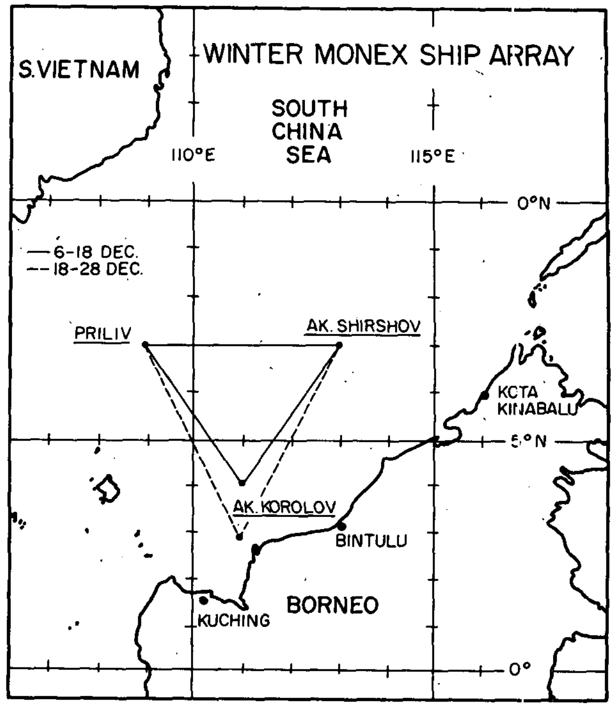

FIG. 2. The Winter MONEX ship observation network during the December 1978 Field Phase.

3. Analysis of heat and moisture budgets

a. Budget equations

Averaging the thermodynamic energy and water vapor equations over the triangle area in Fig. 2 (designating this horizontal average by an overbar) yields the following expressions:

$$Q_1 \equiv \frac{\partial \bar{s}}{\partial t} + \bar{\mathbf{v}}\cdot\nabla\bar{s} + \bar{\omega}\frac{\partial \bar{s}}{\partial p}$$

$$= -\frac{\partial}{\partial p}\overline{\omega' s'} + \bar{Q}_s + \bar{Q}_R, \qquad (1)$$

$$Q_2 \equiv -L\left(\frac{\partial \bar{q}}{\partial t} + \bar{\mathbf{v}}\cdot\nabla\bar{q} + \bar{\omega}\frac{\partial \bar{q}}{\partial p}\right)$$

$$= L\frac{\partial}{\partial p}\overline{\omega' q'} - L\bar{Q}_q, \qquad (2)$$

where $s = c_pT + gz$ is the dry static energy, q the specific humidity, Q_R is the net radiative heating rate, Q_1 is the apparent heat source and Q_2 is the apparent moisture sink. Here Q_s and Q_q are sources of heat and water vapor which may be expressed in terms of individual phase change processes:

$$Q_s = L_v(c - e) + (L_v + L_f)(d - s_*) + L_f(f - m), \quad (3)$$

$$Q_q = e - c - d + s_*, \quad (4)$$

where L_v and L_f are latent heats of vaporization and fusion and c, e, d, s_*, f and m are rates of condensation, evaporation, deposition, sublimation, freezing and melting, respectively. Houze (1982) recently demonstrated the importance of considering ice processes when studying convective heating in tropical mesoscale anvils. For completeness, all possible water phase changes are included in (3) and (4).

The Q_1 and Q_2 measure the net heating and drying effects of convective and radiative processes averaged over the area under investigation. Their vertical profiles have been determined in many regions of the tropics and subtropics for convective systems containing both convective-scale (cumulonimbus) and mesoscale components (e.g., Yanai *et al.*, 1973; Ogura and Cho, 1973; Johnson, 1976; Nitta, 1977). However, until recently (Houze, 1982), there has been no determination of the vertical distribution of Q_1 and Q_2 exclusively for the mesoscale convective components (mesoscale anvils) of tropical cloud clusters.

Houze (1982) has estimated Q_1 for mesoscale anvils by evaluating each term on the right hand side of (1) using information on average anvil cloud structure and precipitation characteristics reported in Leary and Houze (1980). This study takes an alternative approach, namely, to determine Q_1 (and Q_2) from the individual large-scale averaged terms on the left hand side of (1) [and (2)]. A comparison of findings from the two approaches will be made.

b. Data and analysis procedures

Sounding data at each of the three ships in Fig. 2 are generally available at 6-hour intervals; however, some missing and off-schedule releases exist. A list of missing and off-time sounding data for 6–17 December (the time period of the smaller triangular ship array in Fig. 2) is given in Table 1. As mentioned earlier, the convection passed the ship array in early afternoon (1400 LST). Since a considerable fraction of the triangle area was covered by mesoscale anvil clouds only at this observation time (~70%, Johnson and Priegnitz, 1981), we only consider the heat and moisture budgets for 1400 LST. Furthermore, some dates have been excluded from analysis because of missing data at 1400 LST (on the 9th and 11th). Other dates have been excluded because of weak (the 6th) or overly convective conditions (the 13th and 14th) in the ship triangle.

To determine Q_1 and Q_2, the individual terms involving storage ($\partial/\partial t$), horizontal advection ($\bar{\mathbf{v}} \cdot \nabla$) and

TABLE 1. Missing and off-time sounding data during period 6–17 December 1978 for ships *Ak. Korolov*, *Priliv* and *Ak. Shirshov* designated by K, P, and S, respectively. See Fig. 2 for ship positions. Interpretation: K means entire sounding missing at time indicated, S(16) means sounding time 1600 LST, K($P < 629$ hPa) means data missing at pressures less than 629 hPa, etc. No entry at a particular time means soundings at each of the three ships were on time.

	Sounding time (LST)			
Date	0200	0800	1400	2000
6	K		S(16)	
7	K(04)			
8		S		
9			S	
10			K(16)	
11			P($P < 629$ hPa)	
12			K($P < 239$ hPa)	
13	K	K($P < 899$ hPa), S(10)		
14	P, S	K		
15	K	K($P < 909$ hPa)		
16		K(10, $p < 377$ hPa, no winds), P(10)		
17				

vertical advection ($\tilde{\omega}\partial/\partial p$) of s and q must be evaluated. In order to compute these terms in a consistent manner, interpolation in the vertical and in time to fill in the several data gaps that exist is necessary. A procedure was developed and applied that 1) uses a linear interpolation of the fields in time and in pressure at each ship, 2) removes the normal diurnal signal prior to interpolation and reinserts it afterward and 3) matches interpolated with nonmissing data smoothly near the endpoints of the gaps.

Local changes of s and q were computed using centered differences with data 6 h either side of the central time. Horizontal advection was determined by fitting a plane surface to s, q, u and v at the three ship positions. Despite the unavoidable limitations of these procedures, the impact of errors on Q_1 and Q_2 are judged not to be significant since under the convective conditions at 1400 LST the vertical advection terms in the heat and moisture budgets dominate, as has been demonstrated in many other tropical budget studies (e.g., Thompson *et al.*, 1979). Having a more important effect on Q_1 and Q_2 is the procedure used to determine the vertical velocity $\tilde{\omega}$. Here two procedures were tested: 1) balancing by the method of O'Brien (1970), and 2) adding a constant correction term to the divergence (e.g., Johnson, 1976). O'Brien's method assumes that the error in the computed divergence increases linearly from zero at the surface. Procedure 2) was chosen for this study, however, for two reasons: 1) some errors in the wind fields at the lowest levels are anticipated due to problems such as initial locking-in with the sonde transmitter signal and 2) the balloon drift is not large in this region where the average tropospheric wind is ≤15 m s^{-1}. Sensitivity of the results to these procedures is minimal as will be shown later. The alternative approach of applying no correction at all in the computation of $\bar{\omega}$ was discussed in Johnson (1982). There it was seen that with the boundary condition $\bar{\omega} = 0$ at the ocean surface, variations in the computed $\bar{\omega}$ of up to ~30% in the upper troposphere can occur, a situation not uncommon with the application of the kinematic method (O'Brien, 1970).

While radar data are available to describe the nature of the convection as it developed during the morning near the coast of Borneo (Houze *et al.*, 1981), no useful radar data exist to determine the structure of the convection later at midday when it crossed the southern portion of the ship array. The lack of radar data over the ship triangle at 1400 LST precludes any precise determination of the morphology of the convective systems at that time. In general, it is felt that the life cycle of the mesoscale system depicted in Fig. 1 was valid on most days judging from satellite data. Despite the fact that some cumulonimbus convection may have occurred over the triangle at 1400 LST, it is assumed (except on the excluded days 13 and 14 December) that vertical motion was occurring predominantly on the mesoscale. This point is important since we interpret the results to follow to apply primarily to bulk vertical mass flow in the mesoscale anvil.

4. Results

In this section the results presented are based on computations of ω using a constant correction to the divergence. Some comparison with results using O'Brien's (1970) scheme will also be shown.

a. Vertical motion

An extensive analysis of the vertical motion over the ship array is given in Johnson (1982). We will not repeat the detailed results of that study; however, the general character of the vertical motion will be mentioned briefly by reference to the evolution over the course of one day during Winter MONEX.

In Fig. 3 $\bar{\omega}$ is shown for 10 December 1978 at 6-hour intervals beginning at 0200 LST. Satellite pictures corresponding to the four times on this date were presented in Johnson and Priegnitz (1981). Estimates of the fraction of the total triangle area covered by high-level cloudiness using Japanese geostationary meteorological satellite (GMS) infrared (IR) data are indicated at each time in Fig. 3. These cloud amounts are interpreted as high clouds associated with mesoscale anvils and/or cumulonimbus. At 0200 LST no high clouds existed and the vertical motion is relatively weak. By 0800 LST the cloud system covered only a small portion (19%) of the

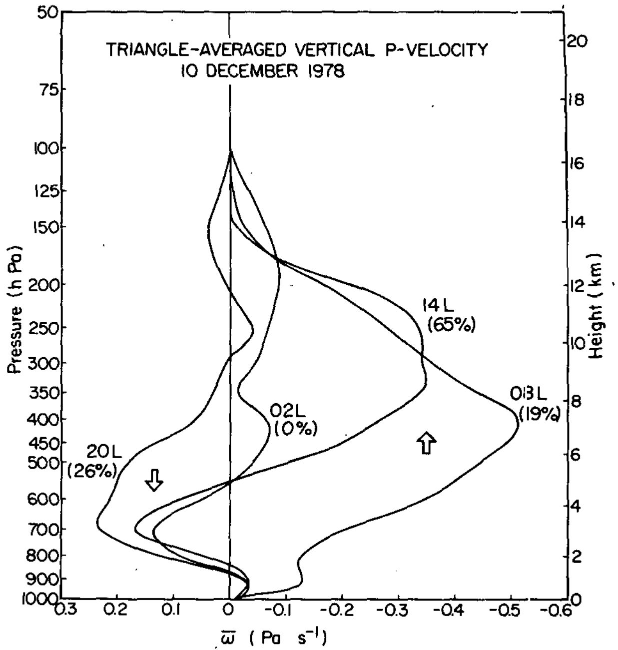

FIG. 3. Triangle-averaged vertical p-velocity $\bar{\omega}$ at 0200, 0800, 1400, and 2000 LST on 10 December. Numbers in parentheses are fractions of triangle area covered by high-level IR cloudiness.

southern part of the triangle and at this time the convection is likely a combination of cumulonimbus and mesoscale anvil features. The computed $\bar{\omega}$ shows a single upward peak near 400 hPa (Fig. 3), a profile consistent with those observed during the mature stage of tropical cloud clusters in many regions of the tropics (Reed and Recker, 1971; Yanai *et al.*, 1973; Nitta, 1977). Six hours later at 1400 LST the profile of $\bar{\omega}$ had changed to one of upward motion in the upper troposphere above the 0°C level (near 550 hPa) and sinking below. This structure has been identified as that associated with the mesoscale anvil clouds, namely, a mesoscale updraft within the cloud and a mesoscale downdraft below (Brown, 1979; Gamache and Houze, 1982; Johnson, 1982). At this time it might be expected that the triangle-computed $\bar{\omega}$'s represent the area-averaged anvil motions quite well since 65% of the area was estimated to be covered by anvil cloud. The mesoscale anvil six hours later had dissipated considerably (Johnson and Priegnitz, 1981), and $\bar{\omega}$ at 2000 LST shows mostly downward motion. This sequence of $\bar{\omega}$ over the life cycle of the mesoscale convective system is quite similar to that depicted and discussed in several other recent studies of tropical cloud clusters (Nitta, 1977; Frank, 1978; Betts, 1978; Houze, 1982).

b. Components of the heat budget

As mentioned earlier, the terms $\bar{\omega}\partial\bar{s}/\partial p$ and $\bar{\omega}\partial\bar{q}/\partial p$ are the primary contributors to the budgets for Q_1

and Q_2. This finding is illustrated in Fig. 4. At 1400 LST 10 December, as on other days at this time, Q_1 closely follows $\bar{\omega}\partial\bar{s}/\partial p$. Storage and horizontal advection of s are comparatively small throughout most of the troposphere. The budget for Q_1 on other days as well as that for Q_2 (not shown) yields the same qualitative conclusion.

c. Q_1 and Q_2 budget results

The Q_1 profiles at 1400 LST obtained for the passage of seven mesoscale anvils across the ship array during December are shown in Fig. 5. On these days an average of 68% of the triangle area was covered by bright IR cloudiness. A table in the figure shows the actual amounts on individual days. Indicated in Fig. 5 is a range estimate for the mesoscale anvil tops based on several reported values using aircraft photogrammetry (Warner, 1981, 1982) and satellite IR brightness values (Johnson and Kriete, 1982). Two major features stand out in Fig. 5: 1) a large positive heat source in the upper troposphere and 2) a region of negative Q_1 in the lower troposphere. The upper tropospheric maximum is primarily a consequence of latent heating (condensation and freezing) in the anvil cloud according to Houze (1982), who has given estimates of the contributions of the various possible physical processes in anvil heating. The cooling in the lower troposphere is largely due to precipitation evaporation and melting (Houze, 1982). Radiative effects are determined by Houze to play a secondary role in the total heating.

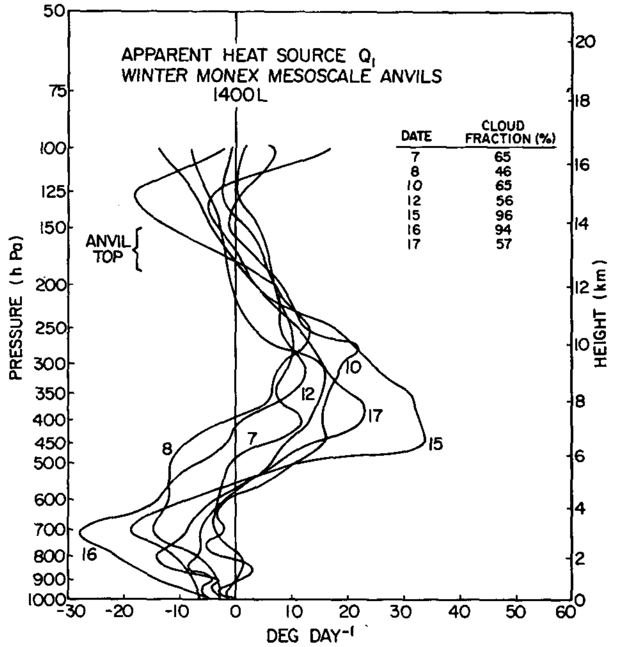

FIG. 5. Apparent heat source Q_1 at 1400 LST on seven days in December. Fraction of triangle area covered by bright IR cloudiness is indicated for each date. Estimate of anvil top level is based on aircraft and satellite data.

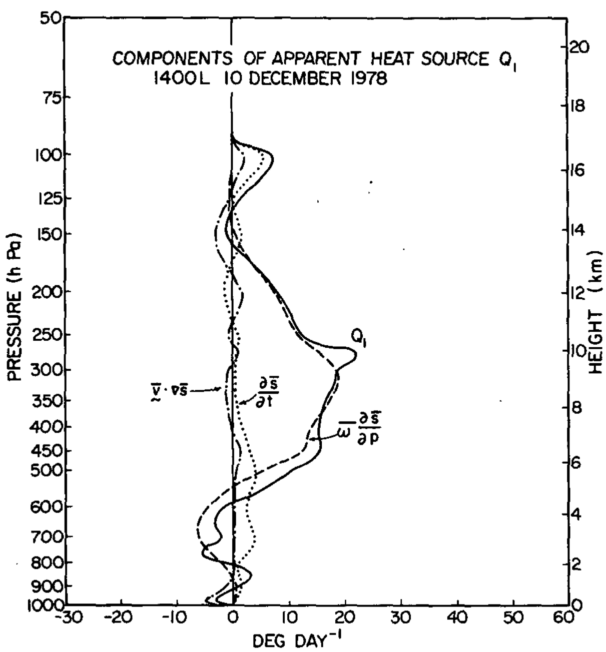

FIG. 4. Components of apparent heat source Q_1 at 1400 LST on 10 December.

A composite or average profile of Q_1 is given in Fig. 6. It has been constructed by drawing a smooth curve through the mean values at the levels indicated by standard deviations. As is evident from Fig. 5, a warming peak is centered near 350 hPa or 8–9 km. This position is approximately 100 hPa or ~2 km below the peak in $\bar{\omega}$ (Johnson, 1982). The location of the peak in Q_1 at a lower level than that for $\bar{\omega}$ is due to the somewhat greater stability ($\propto \partial\bar{s}/\partial p$) near 350 hPa than that near 250 hPa (Fig. 4, Johnson and Kriete, 1982). In the lower troposphere there is cooling with a peak near 700 hPa or 3 km. The transition from warming to cooling near the 0°C level supports the interpretation given above for the maintenance of the mesoscale downdraft. Also indicated in Fig. 6 are composite values of Q_1 obtained by application of O'Brien's (1970) balancing procedure. It is clear that the results here are not very sensitive to the choice of the ω-balancing procedure.

At levels near and slightly above the estimated anvil top there is some indication of cooling. Since latent heating effects should be quite small at these high levels, this cooling may be direct evidence of longwave radiative cooling off the tops of the mesoscale anvils, although the findings are not conclusive. At 1400 LST it is possible that shortwave heating may largely offset the longwave cooling with the net radiative heating being rather weak (Cox and Griffith, 1979; Webster and Stephens, 1980). The cooling discussed here in the layer 100–150 hPa is centered at

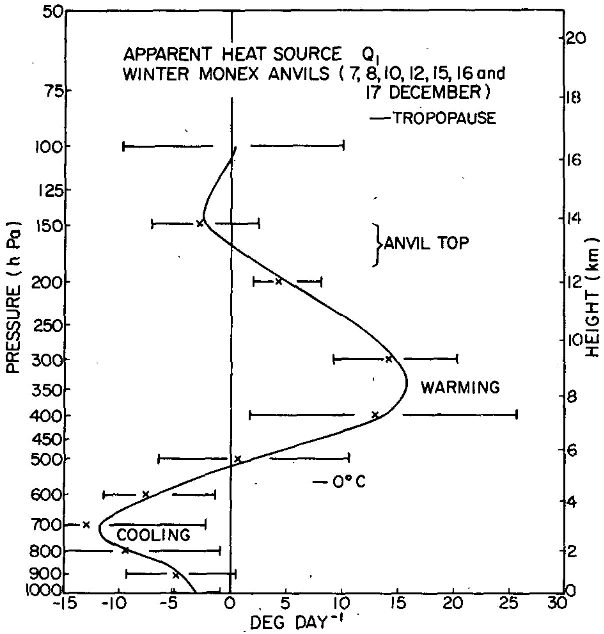

FIG. 6. Composite apparent heat source Q_1 for Winter MONEX anvils. Crosses refer to results using O'Brien's (1970) procedure to balance ω. Horizontal bars indicate standard deviation, computed from data of Fig. 5.

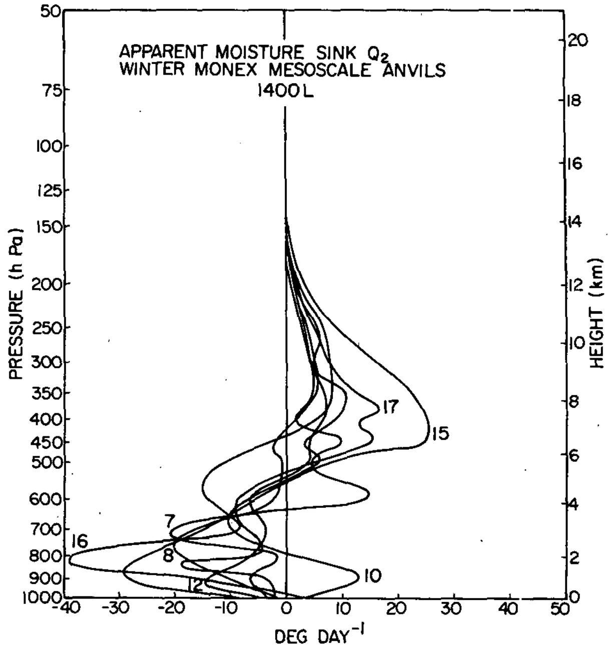

FIG. 7. Apparent moisture sink Q_2 at 1400 LST on seven days in December.

a somewhat lower level than that reported by Johnson and Kriete (1982), based on a sounding time section at the southernmost ship *Ak. Korolov.* Johnson and Kriete found significant cold anomalies (~6°C) near the tropopause (~17 km) extending into the lower stratosphere accompanying the passage of the mesoscale anvils. We attempted an analysis of the Q_1 budget at these higher levels; however, because of the variable tropopause heights between ships and consequent large temperature gradients near the tropopause, very large and erratic Q_1 values were obtained. It is felt that the Q_1 budget can only be reliably interpreted below ~150 hPa (~14 km).

The actual heating rates of Q_1 shown are not meaningfully compared to, say, heating rates associated with cumulonimbus clouds unless the profiles are normalized with respect to rainfall rates. A consideration of this point will be given later when comparisons are made with the findings of Houze (1982).

The individual profiles of Q_2 ($Q_2 > 0$ indicates a moisture sink) for the seven days are shown in Fig. 7. A scatter similar to that for Q_1 is apparent with a pronounced moisture sink (due to condensation and deposition) in the upper troposphere and moisture source (due primarily to evaporation) in the lower troposphere. The profiles appear somewhat more irregular due to the greater variability of q in the region of convection than s. The composite Q_2 profile (Fig. 8) shows the upper peak near 350 hPa corresponding to 4 g kg day^{-1} drying, and the lower peak of -5 g kg^{-1} day^{-1} (moistening) near 800 hPa. The lower Q_2 peak is shifted downward relative to the lower Q_1 peak because q increases exponentially in p towards the surface whereas s is approximately linear (recall that $\bar{\omega}\partial\bar{q}/\partial p$ and $\bar{\omega}\partial\bar{s}/\partial p$ are the dominant terms in Q_2 and Q_1).

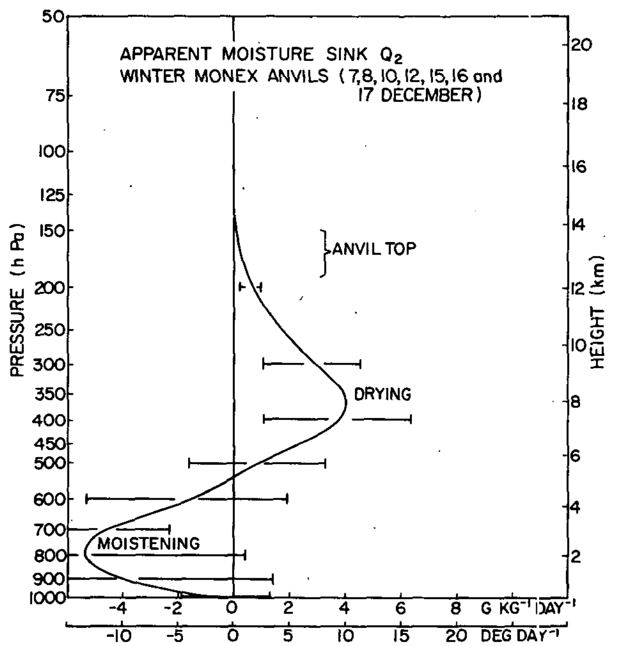

FIG. 8. Composite apparent moisture sink Q_2 for Winter MONEX anvils. Horizontal bars indicate standard deviation.

d. Comparison with Houze (1982)

The profiles of Q_1 and Q_2 are considerably different from those presented in many budget studies for tropical cloud clusters. Such clusters are normally comprised of both cumulonimbus and mesoscale anvil structures. The net heating and moistening by the combined convection is normally computed with no partitioning into its component convective contributions. However, Houze (1982) has shown for the Q_1 budget that the heating given by the mesoscale anvils, warming above and cooling below 0°C, is considerably different from that associated with the cumulonimbus, which gives warming at all levels with a peak in the mid-troposphere. Houze computed Q_1 for an idealized cloud cluster by estimating the magnitude of each of the terms on the rhs of (1) based on previous studies of mesoscale convective systems. His computations were for a mesoscale anvil within a large-scale area A such that the area-averaged rainfall rate over A was 0.5 mm h^{-1}.

In comparing our findings with those of Houze (1982), we choose to exclude the radiative heating component from his total mesoscale anvil heating. This step is taken because: 1) the amplitude of the radiative heating is estimated to be relatively small, except in a thin layer near anvil top (near 10 km, Houze, 1982, Fig. 11), and 2) there is considerable uncertainty in the radiative heating estimates. Point 1) suggests that the qualitative implications of the comparisons will likely not be affected by this procedure.

The comparison with Houze (1982) also requires a determination of the rainfall rate for which Q_1 in Fig. 6 of our study applies. Unfortunately, there is no direct measurement of the average rainfall rates associated with the mesoscale anvils as they crossed the ship array. The best that can be done is to use rainfall estimates determined from the Massachusetts Institute of Technology radar at Bintulu for time periods when the mesoscale anvil was nearer the coastline (Churchill and Houze, 1983). Based on the radar analysis of Churchill and Houze for 10 December, an average rainfall rate for the Winter MONEX anvils of 3 mm h^{-1} is used. This rainfall rate for the stratiform precipitation region was determined on 10 December at a time 3 h prior to the sounding time used in this study. Assuming, as did Houze (1982), that 75% of the bright IR cloudiness associated with the mesoscale anvil is nonprecipitating overhang, then the average 68% cloud fraction for the triangle on the seven days implies $\frac{1}{4} \times 0.68 \times 3$ mm h^{-1} or an 0.5 mm h^{-1} average rainfall rate over the ship triangle area. With this value being equivalent to that given by Houze (1982), we may compare directly then, without normalization, the Q_1 profiles obtained by the two independent approaches. Of course, we must keep in mind that there is considerable uncertainty in both the Winter MONEX rainfall rate and the overhang area estimates given above. These factors, however, only affect the amplitude of the profiles: their shape is independent of these considerations.

The comparison is shown in Fig. 9. The profile shapes as well as the amplitudes are in reasonably good agreement, despite differences in data sets and methodologies of computations. This agreement appears to be mutually supportive of both studies' findings and, further, it can be concluded that the physical hypotheses advanced by Houze (1982) to account for the net heating in the mesoscale anvils may be quite realistic. The general agreement suggests that Houze's estimate of the radiative heating rate, which has this term contributing in a relatively minor way to the total heating, is reasonable.

5. Summary and discussion

An analysis of the heat and moisture budgets for Winter MONEX tropical mesoscale cloud systems has been performed using sounding data from three Soviet research ships during December 1978. On nearly every day during the field phase of the experiment a mesoscale cloud cluster developed along the north coast of Borneo and moved across the ship array during the afternoon. At the time of passage

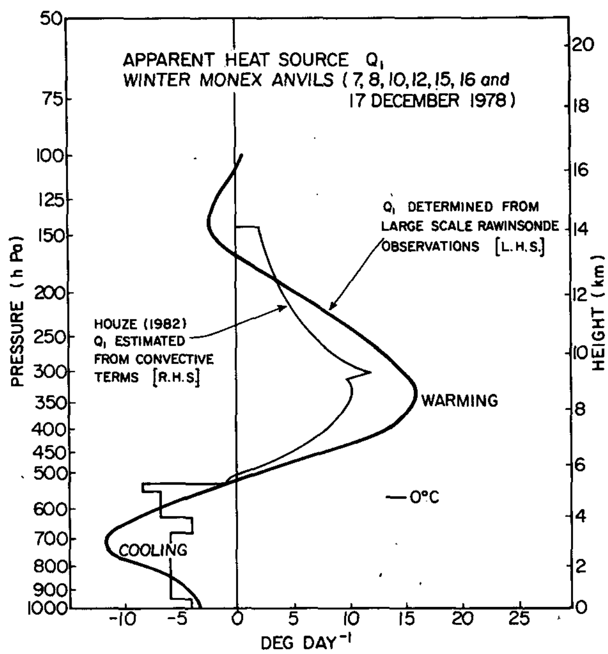

FIG. 9. Comparison of apparent heat source Q_1 obtained from this study using rawinsonde data (heavy curve) with that obtained by Houze (1982, Fig. 9) using radar cloud structure and precipitation data (light curve). L.H.S. (R.H.S.) refers to left hand side (right hand side) of Eq. (1). The curve from Houze (1982) represents the total heating by *non-radiative* mesoscale processes.

over the ships this cloud cluster consisted primarily of a mesoscale anvil cloud (Houze, 1977; Zipser, 1977; Brown, 1979; Houze *et al.*, 1981). Computations of ω by the kinematic method using sounding data from a nearly equilateral triangle of ships formed the basis for further computations of heat and moisture budgets (the apparent heat source Q_1 and apparent moisture sink Q_2).

The primary findings of this study are presented in Figs. 6 and 8 where composite profiles of Q_1 and Q_2 for seven mesoscale anvils are shown. The Q_1 profile shows that diabatic heating in the anvil cloud contributes to give a maximum warming in the upper troposphere near 350 hPa or 8–9 km. This diabatic heating is primarily due to condensation and freezing in the anvil (Houze, 1982). In the lower troposphere rainfall evaporation and melting of frozen hydrometeors contribute to a cooling with a peak near 700 hPa or 3 km. This profile of Q_1 compares quite favorably with that recently derived by Houze (1982) who has taken the opposite approach to solve this problem, namely, to estimate the individual contributions of each of the convective and radiative terms in the heat equation [the rhs of (1)] and then sum them to give a total heating. Both the profile shape and amplitudes of the extrema normalized by rainfall rate (to within acknowledged errors in the precipitation rate estimates) agree rather well.

The composite Q_2 has a shape similar to that of Q_1 with a maximum drying evident in the upper troposphere near 350 hPa or 8–9 km and a maximum moistening by rainfall evaporation in the lower troposphere near 800 hPa or 2 km.

Both Q_1 and Q_2 profiles shown here for mesoscale anvils are considerably different from those determined in many studies for tropical cloud clusters as a whole (e.g., Yanai *et al.*, 1973; Ogura and Cho, 1973; Thompson *et al.*, 1979). In the latter studies Q_1 and Q_2 are both positive throughout the entire troposphere. The shifting of total cluster heating and drying to positive values in the lower troposphere is a consequence of the important contribution of condensational heating in the cumulonimbus clouds to the total cluster heating (Houze, 1982). The cumulonimbus heating, as Houze shows, is a maximum in the mid- to lower troposphere. The partitioning of the heating into cumulonimbus and mesoscale anvil components is done by Houze (1982) using an idealized model for the cloud structures contained within the entire cluster. A worthy objective is to partition the heating from the opposite perspective employed in this study, i.e., the use of large-scale rawinsonde observations. Work in this direction is currently underway. The findings of such a study will be of value for understanding the nature of the physical processes operating within cloud clusters as well as providing a basis for the improvement of methods for parameterizing the effects of convection in large-scale numerical weather prediction models.

Acknowledgments. We thank Machel Sandfort for typing the manuscript. This research has been supported by the Division of Atmospheric Sciences, National Science Foundation under Grants ATM-8015347 and ATM-8206808.

REFERENCES

Anthes, R. A., 1977: A cumulus parameterization scheme utilizing a one-dimensional cloud model. *Mon. Wea. Rev.*, **105**, 270–286.

——, and D. Keyser, 1979: Tests of a fine-mesh model over Europe and the United States. *Mon. Wea. Rev.*, **107**, 963–984.

Betts, A. K., 1978: Convection in the tropics: Meteorology over the tropical oceans. *Quart. J. Roy. Meteor. Soc. (Suppl.)*, 105–132.

Brown, J. M., 1979: Mesoscale unsaturated downdrafts driven by rainfall evaporation: A numerical study. *J. Atmos. Sci.*, **36**, 313–338.

Cheng, C.-P., and R. A. Houze, Jr., 1979: The distribution of convective and mesoscale precipitation in GATE radar echo patterns. *Mon. Wea. Rev.*, **107**, 1370–1381.

Churchill, D. D., and R. A. Houze, Jr., 1983: Development and structure of winter monsoon cloud clusters on 10 December 1978. *J. Atmos. Sci.* (submitted to).

Cox, S. K., and K. T. Griffith, 1979: Estimates of radiative divergence during Phase III of the GARP Atlantic Tropical Experiment: Part II. Analysis of the Phase III results. *J. Atmos. Sci.*, **36**, 586–601.

Frank, W. M., 1978: The life cycles of GATE convective systems. *J. Atmos. Sci.*, **35**, 1256–1264.

Fritsch, J. M., and J. M. Brown, 1982: On the generation of convectively driven mesohighs aloft. *Mon. Wea. Rev.*, **110**, 1554–1563.

Gamache, J. F., and R. A. Houze, Jr., 1982: Mesoscale air motions associated with a tropical squall line. *Mon. Wea. Rev.*, **110**, 118–135.

Hartmann, D. L., H. H. Hendon and R. A. Houze, Jr., 1983: Some implications of the mesoscale circulations in cloud clusters for large-scale dynamics and climate. Submitted to *J. Atmos. Sci.*, **41** (in press).

Hobbs, P. V., 1978: Organization and structure of clouds and precipitation on the mesoscale and microscale of cyclonic storms. *Rev. Geophys. Space Phys.*, **16**, 741–755.

House, R. A., Jr., 1977: Structure and dynamics of a tropical squall-line system observed during GATE. *Mon. Wea. Rev.*, **105**, 1540–1567.

——, 1982: Cloud clusters and large-scale vertical motions in the tropics. *J. Meteor. Soc. Japan*, **60**, 396–410.

——, and A. K. Betts, 1981: Convection in GATE. *Rev. Geophys. Space Phys.*, **19**, 541–576.

——, and P. V. Hobbs, 1982: Organization and structure of precipitating cloud systems. *Advances in Geophysics*, Vol. 24, Academic Press, 225–315.

——, C.-P. Cheng, C. A. Leary and J. F. Gamache, 1980: Diagnosis of cloud mass and heat fluxes from radar and synoptic data. *J. Atmos. Sci.*, **37**, 754–773.

——, S. G. Geotis, F. D. Marks and A. K. West, 1981: Winter monsoon convection in the vicinity of North Borneo. Part I: Structure and time variation of the clouds and precipitation. *Mon. Wea. Rev.*, **108**, 1595–1614.

Johnson, R. H., 1976: The role of convective-scale precipitation downdrafts in cumulus and synoptic scale interactions. *J. Atmos. Sci.*, **33**, 1890–1910.

——, 1980: Diagnosis of convective and mesoscale motions during Phase III of GATE. *J. Atmos. Sci.*, **37**, 733–753.

——, 1982: Vertical motion in near-equatorial winter monsoon convection. *J. Meteor. Soc. Japan*, **60**, 682–690.

——, and D. C. Kriete, 1982: Thermodynamic and circulation characteristics of winter monsoon tropical mesoscale convection. *Mon. Wea. Rev.*, **110**, 1898–1911.

——, and D. L. Priegnitz, 1981: Winter monsoon convection in the vicinity of North Borneo. Part II: Effects on large-scale fields. *Mon. Wea. Rev.*, **109**, 1615–1628.

Leary, C. A., and R. A. Houze, Jr., 1979: The structure and evolution of convection in a tropical cloud cluster. *J. Atmos. Sci.*, **36**, 437–457.

——, and ——, 1980: The contribution of mesoscale motions to the mass and heat fluxes of an intense tropical convective system. *J. Atmos. Sci.*, **37**, 784–796.

Nitta, T., 1977: Response of cumulus updraft and downdraft to GATE A/B-scale motion systems. *J. Atmos. Sci.*, **34**, 1163–1186.

O'Brien, J. J., 1970: Alternative solutions to the classical vertical velocity problem. *J. Appl. Meteor.*, **9**, 197–203.

Ogura, Y., and H.-R. Cho, 1973: Diagnostic determination of cumulus cloud populations from observed large-scale variables. *J. Atmos. Sci.*, **30**, 1276–1286.

Reed, R. J., and E. E. Recker, 1971: Structure and properties of synoptic-scale wave disturbances in the equatorial western Pacific. *J. Atmos. Sci.*, **28**, 1117–1133.

Thompson, R. M., Jr., S. W. Payne, E. E. Recker and R. J. Reed, 1979: Structure and properties of synoptic-scale wave disturbances in the intertropical convergence zone of the eastern Atlantic. *J. Atmos. Sci.*, **36**, 53–72.

Warner, C., 1981: Photogrammetry from aircraft side camera movies: Winter MONEX. *J. Appl. Meteor.*, **20**, 1516–1526.

——, 1982: Mesoscale features and cloud organization on 10–12 December 1978 over the South China Sea. *J. Atmos. Sci.*, **39**, 1619–1641.

Webster, P. J., and G. L. Stephens, 1980: Tropical upper-tropospheric extended clouds: Inferences from Winter MONEX. *J. Atmos. Sci.*, **37**, 1521–1541.

Yanai, M., S. Esbensen and J. H. Chu, 1973: Determination of bulk properties of tropical cloud clusters from large-scale heat and moisture budgets. *J. Atmos. Sci.*, **30**, 611–627.

Zipser, E. J., 1977: Mesoscale and convective-scale downdrafts as distinct components of squall line structure. *Mon. Wea. Rev.*, **105**, 1568–1589.

——, R. J. Meítin and M. A. LeMone, 1981: Mesoscale motion fields in association with a slow-moving GATE convective band. *J. Atmos. Sci.*, **38**, 1725–1750.